Modelling the impact testing of prescription lenses

P. J. McAULIFFE*, R. W. TRUSS* M. PITTOLO†
*Dept. of Mining and Metallurgical Engineering, The University of Queensland, Queensland, 4072, Australia
†SOLA International Holdings Ltd., Sheriffs Road, Lonsdale, South Australia 5160, Australia

Lenses are tested in an impact test in which a steel ball is dropped from a height onto the centre of the lens. This causes the lens to deform until the stress in the lens reaches a point at which fracture occurs. A survey of the literature was carried out and analytical models of the load/deflection and of the deflection/stress relationships were selected. A mathematical model of the impact test on lenses was developed. This model consisted of calculating the load–deflection relationship of a lens loaded at a central point, combined with calculating the deflection at which fracture occurred. From this model the impact energy required to deform a lens to fracture was obtained. This was held to be equal to the minimum kinetic energy of an impactor, less losses, that would be needed to cause lens fracture. As the losses are small, the calculated energy was used as an estimate of the impact strength of the lens. These values were then compared to those established by experiment. The impact energies predicted by the model were a close approximation of the experimental results for the lenses tested.

1. Introduction

This work is part of a project studying the fracture of ophthalmic lenses. Lenses are made in the shape of shallow, partial spherical shells, as shown in Fig. 1. The current method of evaluating the impact resistance of the lenses is to drop balls of varying weights onto the lenses from a height of 50 inches (1270 mm). By varying the weight of the ball, the impact energy required to cause fracture can be determined. This technique is based on the United States FDA Impact Resistance Regulation [1]. This method is expensive in time and materials, and the results are subject to variation due to the natural distribution of flaws in the lenses. These factors make this test unsuitable for use in the development of new materials or lens types.

A major aim of this project was to be able to predict the critical impact energy of a given lens without the time and expense of constructing a die, casting a series of lenses and then testing a sufficient number of lenses to establish a statistically valid result. To this end a model was created of the impact situation which was used to predict the impact energy from easily measured properties such as fracture stress and Young's modulus.

The model was initially developed for plano lenses, an industry term meaning that the lens thickness was constant. This gives a lens that does not have any refracting power, such as those used for sunglasses and safety goggles. Constant lens thickness simplified calculation but as the majority of production involves prescription lenses which have varying wall thickness, the model was also extended to prescription lenses.

2. Modelling

2.1. Failure criteria

The standard FDA impact test for ophthalmic lenses consists of placing a lens on a circular support 25.4 mm in diameter with the convex side uppermost. The steel ball is dropped from a height of 1270 mm, giving an impact velocity of 5 ms^{-1}. The drop weight impacts the lens in the centre of the convex side and causes the lens to deform. This deformation causes stress in the lens, and when the stress reaches the failure stress of the lens material, the lens will break.

Because the lens materials are brittle, the failure occurs by fast fracture. Fracture occurs when the stress reaches a level where a flaw or crack that is already present in the sample is able to grow so that the sample breaks. This situation is represented by

$$K_{1c} = Y\sigma\sqrt{\pi a} \quad (1)$$

where K_{1c} is the critical stress intensity factor at which a crack will grow in the material, Y is a factor related to the geometry of the crack, σ is the stress and a is the length of the crack.

The stress at which crack growth occurs is determined by the K_{1c} of the material and the size and distribution of flaws within the sample. The approach adopted in this work was to measure the stress at failure using a simple mechanical test and to use this value to calculate the impact strength. The failure stress was measured using a sample in bending. Since the failure region of the lens in the impact test was also in bending, the use of bending samples gave similar

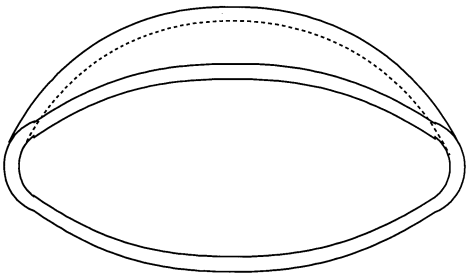

Figure 1 Pictorial view of an ophthalmic lens.

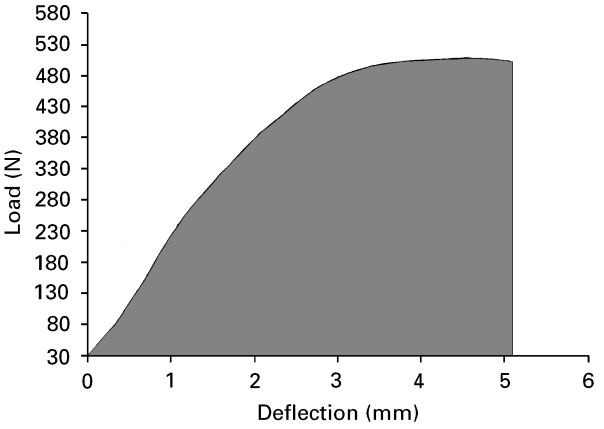

Figure 2 A typical load versus deflection curve showing the stored elastic energy.

flaw geometry to the impact test. Hence the geometry factor Y should be the same. Moreover, the fracture stress samples were cut from lenses, which ensured that the size and distribution of the flaws was identical to those causing failure in the lenses under impact.

Therefore, the failure stress of the lens material measured in the simple bend test should give a reasonable estimate of the failure stress of the lens during impact provided the test material does not show a strong rate dependence in its mechanical properties. This point will be discussed later.

2.2. Modelling a plano lens

2.2.1. Energy transfer

If the failure stress of a lens is known, it is now possible to calculate the deflection of a lens at the point of fracture in the impact test. Initially a model was developed for a plano, uncoated lens that was impacted in the centre of the convex side by a sphere with a known kinetic energy. The inertial effects of the lens were neglected, and the stress/strain relationships were treated as quasistatic. Impact behaviour can be treated as if the load was applied quasistatically if the speed of an impact is low enough to avoid significant energy loss through factors such as vibration, noise, heat and the kinetic energy of fragments [2].

Assuming that the lens behaves elastically under impact loading, the maximum deflection of the lens at the point of load application (Δ) will be such that the stored elastic energy in the lens is equal to the kinetic energy (E_k) of the drop weight. Hence:

$$E_{\mathrm{k}} = \int_0^{\Delta} P \, \mathrm{d}\delta \qquad (2)$$

where P is the load on the lens and δ is the deflection caused by that load.

This stored energy is represented as the area under the load/deflection curve for the lens as in Fig. 2.

2.2.2. Lens deflection

Observation of the compression of a lens shows that the deflections reached were large when compared to the thickness of the shell. Hence, the linear stress/strain relationships, such as those listed by Roark [3], were invalid. However, if the load/deflection curve and the deflection at which failure occurs are known for the lens, then it would be possible to integrate the load/deflection curve up to that point to obtain the kinetic energy required to fracture the lens.

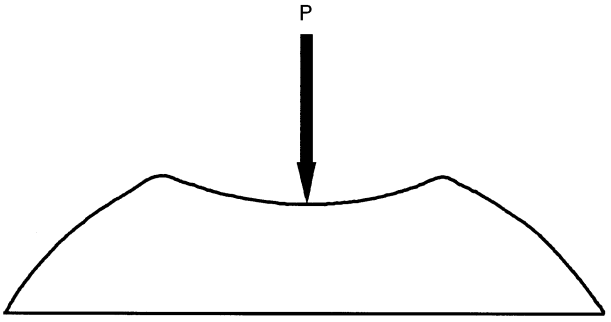

Figure 3 The shape of a spherical shell buckling under a central point load.

The literature has very few references [4–8] that discuss large deflections of a thin, shallow, spherical shell under point loading. The deflection of the lens can be summarized as follows. The shell undergoes a limited amount of linear elastic deflection as described by Roark [3] before the shell begins to buckle. This buckling process consists of the top of the shell turning inside out and producing a section of shell, concentric with the indentor, that has its curvature reserved [4, 6], as shown in Fig. 3. As the walls of the shell are thin, the amount of strain in the reversed section is very small, approaching zero as the wall thickness approaches zero. The sources of strain in the shell walls are the linear deflection as described by Roark [3] and the sharp curvature at the boundary between the reversed and unreversed sections of the shell.

Buckling of this spherical shell has been studied by Pogorelov [4], Chien and Hu [5], Ashwell [6], Biezene and Grammel [7], and Leckie [8]. Analysis of the buckled shell consists of calculating the strain energy in the deformed shell and comparing this with the amount of work done in deforming the shell. The differences between the separate approaches in the literature consist of the assumptions made about the shape of the boundary between the inverted inner region and the outer region, and the approximations used in finding the solutions to the strain equations.

The final solutions to these approaches tend to be similar in form [5–8] except for that derived by Pogorelov [4]. In his solution, the deflection of the point of load application (δ) is given by

$$\delta = \frac{R^2 P^2}{9\pi^2 c^2 E^2 t^5} \tag{3}$$

where R is the radius of curvature of the undeformed shell, c is a constant ≈ 0.19, E is the modulus of the material, and t is the shell wall thickness. It can be seen that this solution gives a value of force that is constantly increasing with deflection. However, as will be seen later, the experimental values of the load on the lenses in this work increased up to a peak load and then decreased. Pogorelov's approach was clearly unable to model the experimentally determined lens behaviour.

The solutions given by Chien and Hu, Ashwell and Biezene and Grammel all correctly model a peak in load, but disagree as to the position of the actual peak (see Fig. 5). The solutions are given in the form of curves which represent the equations expressed in the form of dimensionless parameters. For Ashwell [6] and Biezene and Grammel [7] these consisted of P' plotted against δ' where

$$P' = \frac{PR}{Et^3} \tag{4}$$

and

$$\delta' = \frac{\delta}{t} \tag{5}$$

Chien and Hu [5] used a different dimensionless parameter for the load. Their parameter was Q where

$$Q = \frac{2fbr^2}{Et^4} \tag{6}$$

where f is the height of the lens, b is the radius of the circle on which the load is applied and r is the radius of the lens. Chien and Hu [5] then developed a polynomial that related Q to δ/t.

$$Q = (0.66 + 0.08368k^2)\frac{\delta}{t} - 0.255k\left(\frac{\delta}{t}\right)^2 + 0.1734\left(\frac{\delta}{t}\right)^3 \tag{7}$$

where $k = 2P/t$.

Unfortunately, their Equation 7 for the dimensionless load parameter is not dimensionless and has no relation to the load. This is most probably attributable to misprints in the translation of their paper. If f is assumed to be the load (P) instead of the lens height then their equation matches their description and the resulting curve approximates those of Ashwell [6] and Biezene and Grammel [7].

2.2.3. Modelling the stress in the lenses

To allow for the large deflections encountered in the lenses (see Fig. 3) the lens was modelled as a simply supported, circular plate subject to a large deflection because of a central point load. This approximation is valid because the ratio of lens height to lens diameter is less than 1/8 [9]. The stress in the centre of such a plate is given by Blake [2] as

$$S = F(\delta, t)\, E \frac{t^2}{R^2} \tag{8}$$

where F is a function of δ and t.

2.3. Modelling prescription lenses

2.3.1. Initial assumptions

In the deformation of a partial spherical shell, the deflection consists of two parts. The first part consists of the linear deflection with no large change in the overall shape of the lens as described by Roark [3]:

$$\delta = \frac{-\,A P r^2\, 12\sqrt{1-\nu^2}}{16\,\pi\, Et^3} \tag{9}$$

where ν is the Poisson's ratio and A is a variable dependent upon the geometry of the shell. The second part of the deflection consists of buckling. In this case the deformation occurs in a circular hinge that forms concentrically to the axially applied load. This form of deflection is generally larger than the first sort.

From this behaviour, a hypothesis was proposed for the deflection of a powered lens. This was that at a given load P, the centre of a powered lens will have a deflection due to buckling equal to that of a plano lens of the same radius and of thickness t, where t is the thickness of the powered lens at the radius of the buckling.

2.3.2. Allowing for linear deflection

The above hypothesis did not take into account the linear deflection of the inner portion of the lens. The inner portion was the region of the lens that was inside the hinge line when buckling occurs. This linear deflection was larger for a concave lens as it becomes thinner towards the centre, where most of the deflection occurred. Likewise a convex lens had less linear deflection than a plano lens.

The linear deflection of a shallow spherical shell has been described by Roark [3]. This equation is for a shell of constant thickness. For a shell of variable thickness, a different approach was required.

In this case, the central area of the shell was broken up into a series of concentric rings. Each one of these rings was given a constant thickness corresponding to the thickness of the shell at that radius. The rings were assumed to be constrained at the ends to approximate the fact that they were joined onto the next ring segment. For each ring the deflection was calculated and these were summed to give the total deflection for the inner portion of the lens.

The linear deflection calculated for the prescription lens was then used to correct the deflection previously calculated for the plano lens with the same amount of buckling. This gave the total deflection for the prescription lens.

2.4. Calculating the impact energy

To calculate the deflection of a prescription lens, it was easier to start with the deflection and calculate the load. Therefore a row of deflection values were set up in a spreadsheet. From these values the load could be calculated as follows.

Given a deflection (δ), the radius of the hinge line (r') and hence the thickness at the hinge (t) were calculated. With the values of δ and t, the load P was calculated using the same formula as for the buckling of a plano lens. Using the load, the value of δ was corrected to allow for the elastic deflection of the inner region, as described above, and from the new δ, the stress (σ) was calculated. With the final values of δ and P, the incremental strain energy was obtained. The incremental strain energies were then summed until the stress was equal to the breaking stress of the material. The sum of the strain energies should then have been equal to the kinetic energy required to break the sample.

3. Experimental procedure

3.1. Materials

The materials used in this study were proprietary thermosetting resins supplied by SOLA International Holdings Ltd., and designated R1, R2, R3 and R4:

R1 was a poly-diallyl diethylene glycol carbonate.

R2, R3 and R4 are proprietary thermoset materials supplied by SOLA.

3.2. Modulus of rupture tests

3.2.1. Modulus of rupture principles

To provide a measure of the fracture stress of the material, a modulus of rupture (MOR) test was used. This consisted of a test whereby a strip of the material to be tested was placed in three-point bending as shown in Fig. 4. The load on the sample was increased until failure occurred in the tensile (for brittle materials) face of the specimen. The stress (σ) at failure can then be calculated by

$$\sigma = \frac{My}{I} \tag{10}$$

where M is the applied bending moment at failure, y is the distance from the neutral axis to the tensile face and I is the moment of area of the sample cross-section.

For a flat strip the modulus of rupture is equal to

$$\sigma = \frac{3PW_m}{bt^2} \tag{11}$$

where P is the load at failure, W_m is the length of the moment arm, b is the width of the strip and t is the strip thickness.

For brittle materials, the failure was in the form of catastrophic crack growth from some flaw that was on or near the tensile face in the region of maximum stress, i.e. beneath the central loading line.

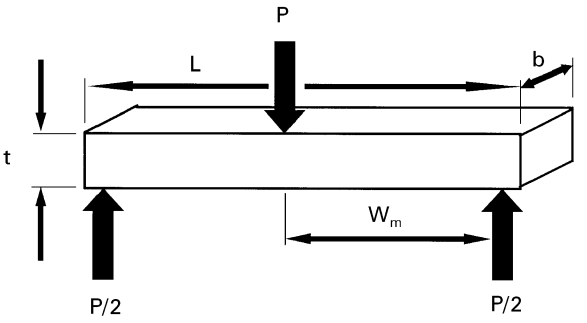

Figure 4 A modulus of rupture sample showing the applied loads.

3.2.2. Sample preparation

30 mm wide strips were cut from the centre of each lens with a hacksaw. The strips were then cut into halves, giving specimens 30 mm wide by 35 mm long. This gave a sample of the required size but with very rough edges. As the sample was required to fail from a flaw that was present in the as-received material, the potential failure sites in the edges had to be removed before testing. This was done by using a series of successively finer grades of abrasive paper on a polishing wheel, finishing with diamond paste of 1 μ grade to give a fine polish. This ensured that the flaws causing the failure were the original flaws in the surface of the lens.

3.2.3. Testing procedure

The strips were placed, convex side up, on two supporting edges 25 mm apart. The load was then applied via a central line. This rig was then loaded in an Instron model 1026 testing machine until the sample failed. The test was performed at a crosshead speed of 10 mm/minute at a temperature of 25 °C. A complete plot of load versus extension enabled the bending moments to be calculated. From these, the modulus of rupture could be evaluated.

Similar tests were then performed at strain rates between 1 mm/minute and 500 mm/minute to determine the effect of changes in strain rate.

3.3. Single-point compression of lenses

To test the lenses quasistatically, the lenses were compressed at a crosshead speed of 10 mm/minute under a 16 mm (5/8 inch) spherical indentor applied to the centre of the convex side. The lenses were supported on a Teflon® coated annular ring of 25.4 mm (1 inch) diameter. The size of the indentor and the support ring was the same as those specified for the FDA impact test.

The load deflection curves from these tests were compared to those predicted by the models from the literature to find the best match.

3.4. Drop weight tests

The initial drop weight tests were carried out in accordance with the FDA procedure [1]. Lenses

which passed this test were subjected to further impacts of increasing energy (increasing ball weight and height) until failure occurred. The average energy required to cause failure was then calculated. This test was carried out on a variety of plano and prescription lenses.

4. Results

4.1 Load deflection curves

The load deflection curves for the lenses were measured experimentally using the single-point compression test. These curves start with an almost linear rise in load, which gradually plateaus out before decreasing again as the lenses buckled. These curves were then compared to those from the literature. The method from the literature that was found to give the closest approximation to the experimental results was that of Ashwell [6]. An example of this comparison is shown in Fig. 5 for a 3 mm thick plano lens.

4.2 Bend tests

The modulus of rupture and the elastic modulus obtained from the bend tests are given in Table I.

The bend tests carried out at different strain rates showed that there was some dependence of mechanical properties on strain rate but that this relationship is not a strong one. These results correlate with the findings of Frounchi *et al.* [10].

This data was combined with the stress/deflection Equation 8 of Blake [2] into a spreadsheet. From this spreadsheet the theoretical load/deflection curves were calculated from the dimensions of a lens and the elastic modulus. Then, given the rupture stress, the deflection at which fracture would occur was calculated, and hence the impact energy at fracture was obtained.

4.3. Comparison of calculated and experimental results

The impact results for plano lenses from the computer calculations and the experimental results are presented for a variety of different lens types in Table II.

The impact results calculated from the model for powered lenses are shown in Table III compared to experimental results.

5. Discussion

The impact results calculated from the MOR and modulus data were in close agreement with the experimental data, especially those for energies less than one joule. The degree of precision obtained from the computer model was also very good, at least as precise as the multiple drop-weight tests.

There were, however, some deviations from the calculated results, particularly in the lenses with the highest impact resistance. This is because this model did not take into account three important factors.

First, in the single-point compression tests, the lenses did not always deform in the manner predicted by the equations. For those lens shapes that had high

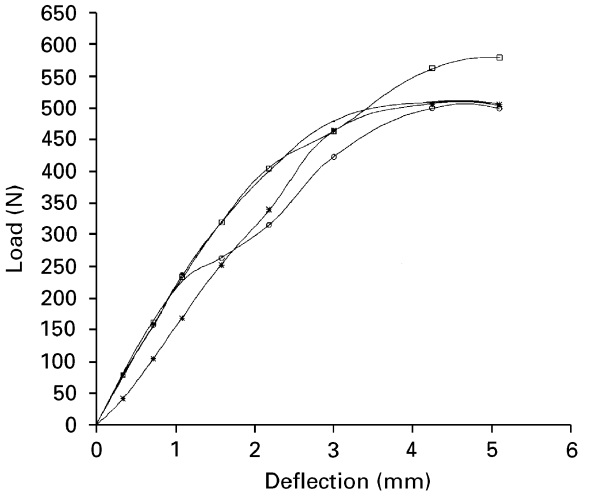

Figure 5 Theoretical load deflection curves (× [6]; ○[7]; □ [5]) compared with the measured values (——).

TABLE I Experimental values of modulus of rupture, or fracture stress

Resin type	Elastic modulus (GPa)	Modulus of rupture (MPa)
R1	1.3	53 ± 3
R2	1.34	70 ± 4
R3	0.97	34 ± 6
R4	1.1	75 ± 6

TABLE II Experimental and predicted impact results for plano lenses made from the different resins

Resin type	Thickness (mm)	Diameter (mm)	Calculated energy (J)	Impact energy (J)
R1	1.8	70	0.65–0.7	0.7
R1	2.0	70	0.8–0.86	1.1
R1	3.0	65	1.38–1.5	1.5–2.8
R2	1.75	70	0.38–0.39	0.4
R2	1.8	70	0.82–0.93	0.7
R2	2.0	70	1.01–1.14	1.2
R2	3.0	65	1.83–2.1	1.7–2.8
R3	1.8	70	0.48	0.26–0.5
R4	2.19	70	0.7	0.6

TABLE III Experimental and predicted impact results for powered lenses

Resin type	Centre thickness (mm)	Front curve/ back curve (dioptres)	Impact energy (J)	Calculated energy (J)
R1	1.8	6.00/6.00	0.7	0.675
R1	1.8	2.50/7.50	1.3	1.2
R2	1.8	6.00/6.00	0.7	0.85
R2	1.75	4.75/4.75	0.4	0.39
R2	1.5	2.00/7.00	1.5	0.9
R2	1.5	4.75/6.00	0.7	0.6
R4	1.25	4.01/6.00	0.29	0.27

impact energies, particularly for those significantly above one joule, the shape of the load/deflection curve deviated substantially from the predicted curve. Both of the original analytical studies were intended to be accurate only within deflection-to-thickness ratios smaller than three [2, 6]. Although most of the lenses tested had maximum deflections below this limit, the 1.5 mm R2 lenses were beyond the capabilities of this model.

Secondly, assumptions were made about the position of the crack initiation point. The model assumed that the critical flaw was located at the surface of the centre of the concave side of the lens, opposite to the impact point. This area of the lens was put into biaxial tension by the deformation of the lens. The flaw itself was very small compared to the size of the wall thickness or the radius of curvature so it was modelled as a surface crack subject to a tensile load due to a bending moment. This is the same situation as the modulus of rupture test. Thus the same fracture stress should apply to both cases. Scanning electron microscopy of the fracture surfaces revealed that fracture did, in fact, originate from surface flaws. However, for samples that failed with a high impact energy, such as the second and fifth entries in Table III, the fracture did not arise from the stress under the impact point. Instead the initial fracture occurred in the hinge line that separated the inverted from the non-inverted regions of the buckled lens. This resulted in the formation of a circumferential crack concentric to the impact site. At this position, the stress in the material was determined by the radius of curvature of the hinge line, and the shear stresses across it. The addition of substantial amounts of shear stress would also have affected the applicable shape factor at the crack tip.

Finally there were the assumptions made about the strain rate dependence of the lens materials. Like all polymers these resins exhibit viscoelasticity [10], but because of their high crosslink density and high glass transition temperature, the effects of strain rate were small over the changes in velocity encountered in this work.

In the development of new resin materials, especially those with higher fracture toughness, it is likely that some resins will be much more sensitive to strain rate effects. In these cases, the values of fracture stress and elastic modulus must be determined at the impact velocities, not at the normal testing rates available in standard laboratory test equipment.

6. Conclusions

The model developed in this work was able to predict the impact energies of ophthalmic lenses in the FDA impact test. From a simple measure of the failure stress and the modulus in bending, the impact energy of any prescription lens could be estimated. The accuracy of the method was limited in those lenses where the impact energy was high as the failure mode changed from failure under the point of impact to failure at the line of buckling. The model also assumed that the strain rate dependence of the mechanical properties was low, which may limit the model for some materials.

References

1. W. M. SNESKO and J. F. STIGI, in "Impact resistant lenses: questions and answers" (HHS Publication (FDA) 87-4002, 1987).
2. A. BLAKE, "Practical stress analysis in engineering design" (Marcel Dekker, New York and Basel, 1990) pp. 410–415.
3. W. YOUNG, "Roark's formulas for stress and strain" (McGraw-Hill, New York, 1989).
4. A. V. POGORELOV, "Bendings of surfaces and stability of shells" (American Mathematics Society, Providence, Rhode Island, 1988) pp. 1–16.
5. CHIEN WEI-ZONG and HU HAI-CHANG, in IX Congrès International de Mecanique Appliquèe, vol. 6 (Universite de Bruxelles, 1957).
6. D. G. ASHWELL, in Proceedings of a Symposium on the theory of Thin Elastic Shells, edited by W. T. Koiter (North Holland, Amsterdam, 1960).
7. C. B. BIEZENE and R. GRAMMEL, "Engineering dynamics: Vol. II" (Blackie, London and Glasgow, 1956) pp. 484–496.
8. F. A. LECKIE, in Theory of Thin Shells, 2nd Symposium, Copenhagen, Sept. 5–9, 1967, edited by F. I. Niordson (Springer Verlag, Berlin and Heidelberg, 1969).
9. V. Z. VLASOV and U. N. LEONT'EV, "Beams, plates and shells on elastic foundations" (Israel Program for Scientific Translations, Jerusalem, 1966) p. 184.
10. M. FROUNCHI, R. P. CHAPLIN and R. P. BURFORD; *Polymer* **35** (1994) 752.

Received 2 October 1995
and accepted 18 September 1996